Evaluation of Active Tectonics in Northwest of Saveh

Bahar Rezaeinahal (baharrezaeinahal@yahoo.com)
Islamic Azad University
Mohsen PourKermani
Islamic Azad University
Mehdy Zare
International Institute of Earthquake Engineering and Seismology
Maryam Dehbozorgi
Kharazmi University
Reza Nozaem
Tehran University: University of Tehran

Research Article

Keywords: Active tectonic, Morphometric indices, Kooshk E Nosrat's fault, Indes fault, Avaj fault, Aipac fault

Posted Date: March 30th, 2021

DOI: https://doi.org/10.21203/rs.3.rs-303169/v1

Abstract

The northwest zone of Saveh city is located in the fault zone of the Indes, Koosh e Nosrat, Avaj and Aipak. Indes faults, Cox Nosrat, Avaj and Aipak are considered as the major faults of central Iran, which are also active in the Quaternary and the last movements of these faults are attributed to the present covenant, therefore, the estimation of morphometri in order to identify the effect of active tectonics on the tectonic evolution of drainage basins seems necessary. Therefore, in this study, six important morphotectonic indexes were analyzed; longitudinal gradient of the river, asymmetry of drainage basin, hypometric integral, Drainage basin shape,the ratio of the width of the floor to the height of the valley and forehead of the mountain is discussed.to create the basins on the studied area, Arc Hydro software (Arc GIS software) has been used based on data from a digital elevation model, Then, 6 morphotectonic indexes have been compiled and classified on each of the basins.Finally, according to which the region has been classified into 4 categories of high, medium and low tectonic activity the, Active Tectonic Index (IAT) has been calculated.According to the IAT index, 5% of the study area shows very high tectonic activity, 25% of the studied area has high tectonic activity, the average tectonic activity has 65% and about 5% of the tectonic activity are low. In this study, the highest level of tectonic activity is in the north-eastern part of the region. In most of the sectors, the level of activity is high and moderate, which is related to the activity of Koshk E Nosrat, Aipak, Avaj faults.

1. Introduction

Central Iran is located in the center of Iran in the form of a triangle that is limited to the Alborz Highlands and a series of down holes and beltways of the direct faults of the Sanandaj-Sirjan Zone. [23] In the whole region of Central Iran, especially in the marginal regions, the intensity of tectonic activities is high due to convergence problems between different zones. [1] - [3] For this reason, further fragmentation and more faults in the central Iran, as a continental margin, are expected. The study area is due to the presence of active faults such as; the Indes and Kooshk E Nosrat are active in terms of seismicity due to the continuity of the Arabic-Iranian convergence. So, in the map of Iran's earthquake hazard zonation, except high and very high risk areas [24], evidence of creeping and displacement of quaternary sediments is confirmed by faults in the region [6]. Access to the region is from the northwest of Saveh, southwest of the city of Karaj, and .... (Figure 2-1)

This area is located in the part of Tabriz-Saveh tectonic zone [1]. Indes, Apeg, Avaj and Noshkad faults in the fault zone are one of the main faults in the region, which are considered as active faults in the Quaternary according to seismic activity and other non-structural activities are observed and they are known as active faults in the Quaternary. To study the effect of recent activity of this fault zone, analysis of drainage basins located on the northwest of Saveh area has been used by morphometric indices. The morphometric characteristics of drainage basins have been extensively studied in many parts of the world [4]and [26]. Therefore, these indicators can be recognized and used as a useful tool in active tectonic reports [20], [22], [28]. Also, the comparison between several morphotectonic indexes with software such as Arc GIS can provide a precise numerical method for determining the tectonic activity of the area [19]. Therefore, for the active tectonics estimation, the study area was extracted using the ArcHydro plug-in ArcGIS software for drainage basins and river basins of each basin (Figure 2). Six important tectonic indexes have been investigated; longitudinal gradient of the river, asymmetry of drainage basin, hypersometric integrals, drainage basin shape ratio, the ratio of the width of the valley to the height of the valley and the index of the mountain forehead. In addition, field operations were performed to determine the accuracy of all indices and observe tectonics related to fault and china landforms and to complete the results of this study, and the results were compared with morphotectonic analysis.

2. Procedures

In order to determine the active tectonics in the drainage basin scale and using morphometric indices in the study, initially, the drainage basins were extracted using the Arc Hydro plugin in Arc GIS 10.1 software and the area was divided into 40 separate basins. Then, the main river network was created in the study area and finally, morphometric indices were measured on the basins formed. To create a drainage network, first we fill the holes in the digitized raw height model, in fact, this hole or wells are defined by cells without a drainage path, and none of the surrounding cells is located below it, the result is a raster output with wells filled. In the next step, the drainage flow was calculated and a lattice outlet from each cell was created relative to its most progressive adjacent cell in the downward direction of the slope.

Then, the accumulation of flow in different points of the digital height model is calculated and a raster output of the accumulated flow for each cell is obtained.

Then this raster file is the accumulated flow change size, this size change is calculated by calculating logarithms based on 10 for all cells in a raster map. In this calculation, flow aggregation is used as input data. In the following, create a flow grid and then determine the flow class to determine which category of drains are located. By doing this, a numerical value was obtained for each piece of line branch. To do this, there are two types of STRAHLER and SHREVE classifications that STRAHLER method is used in this study. In this method, the flow class only increases when other threads with the same category are disconnected.

Therefore, the connection of a first-order stream with a second-order stream, instead of creating a third-level connection, will remain a second-order stream. Finally, in order to extract the river network, the raster file has been converted to a linear network (Fig. 3). Consequently, by using the results of previous steps, 40 drainage basins and their main rivers in the study area were defined by using the Arc GIS 10.1 software (Fig. 3).

Morphometric indices were measured by using digital elevation model and topographic maps that derived from it. In the next step, in order to determine the geological units and the main faults of the region, 1: 100,000 geological map of the area was used and in order to determine the activity of the structural elements of the region in quaternary units such as cones, the IRS P5 satellite image of the Army Geographic Organization has been used. Then the accuracy of the above data has been verified by conducting extensive field studies in all parts of the study area. Finally, the relationship between the quantitative morphometric data measured by the software, the structures obtained from field studies and the lines determined by satellite images in the region has been analyzed and their combination in the region of the final land gravity index (IAT) has been determined and the relative active land development has been determined throughout the study area.

3. Morphotectonic Indices

3.1. Longitudinal river gradient index (SL)

Longitudinal gradient index (SL) is one of the morphometric indices that identifies the relationship between erosion and river flow, this index is also related to the power of the river [15]and [16]. Because of SL's sensitivity to river bed slope changes, this index can be used as an effective and suitable tool for estimating river flow turbulence [29]. The SL index equation is computed by the formula [12]– [14] and [8]:

$SL= (\Delta H/\Delta Lr)\ Lsc$

In the above relation, SL is the longitudinal gradient of the river, (ΔH / ΔLr), the channel gradient of the river and Lsc is the total length of the river channel from the starting point of the index to the highest point of the canal. In addition to the above, for the SL index, this index can also be used to estimate relative tectonic activity [20]. To calculate this

index, a digital elevation model (DEM) with a precision of 30 meters along any flow path and for all the basins in the Arc GIS 10.1 software has been used.Finally, the average values of this index for each sub-basin are also calculated. Here, in order to calculate the SL index for each of the existing floodplains in the 40 sub-basins, the scope is studied. The topographic layers of the digital elevation model with a precision of 30 meters to the layer of streams were added to the Arc GIS 10.1 environment and the values Lsc and (ΔH / ΔLr) were measured. As a result, SL values are smaller than 300 green, 500-300 yellow, 950-500 bright blue, 1550-950 blue, dark blue, 3000-1550 violet, and more than 3000 red [11]. At the end, the channel layers with values of SL index were placed on the digital elevation model and the longitudinal gradient map of the river was studied in the studied area (Fig. 4). According to the prepared map, the highest values of SL in the basins (0, 6, 12, 22 and 29) are measured, which is influenced by the effects of the Kooshk E Nosrat, Hasan Abad, Aipak and Soltanieh faults.

In Figure 5, the map of the distribution of SL anomaly values on different resistance rocks is plotted by recording anomalous values on a geology map of 1: 100,000 digitized (Geological Survey of Iran). Considering the stone nature of the river valleys, the large amounts of the above-mentioned SL anomalies can be interpreted as landmarks. Given the available data and geological map, the high values of the anomaly of the SL index are consistent with the faults of Noshkat and Hasanabad faults.

3.2. Asymmetry of drainage basin (Af)

Drainage Asymmetric Indicator (Af) is used to assess and evaluate the tilting of the basins. The geometric shape of the riverside network can be described quantitatively and quantitatively in several ways. The asymmetric factor of the relationship is computed here:

$Af=100\ (Ar/At)$ [17] , [20]

In the above relation, (Ar), the area to the right of the basin relative to the main river (downstream) and (At) is the total area of the drainage basin. If the result of calculating the drainage asymmetry index is close to 50, it indicates that the basin has a constant condition without a slight tilting or tilting. If the value of this indicator is larger or smaller than 50, then the basin is tilted, and it can be inferred that the basin is affected by the tectonic activity or is influenced by the linguistic characteristics and characteristics of the area. In general, for a drainage network in a basin where there is a continuous flow in a constant state, the value of this index should be 50. This index is related to bending perpendicular to the main drainage in the affected basin.

If more bending is in the opposite direction, Af is less than 50. Most morphotectonic indices provide better results in regions and basins with similar lithological conditions. In calculating the Af index and analyzing the results, the effects of lithological controllers and climatic conditions are not taken into account.

In this study, the drainage basin asymmetric index and the area of the right area of the basin (Ar) and the total area of drainage basin (At) in Arc GIS 10.1 software were calculated and Af index in 40 drainage basins in the study area were studied and measured. The value of this indicator varies from 15 (in basin 6) to 85 (in basin 10). After calculating this index for all basins, the results of these values were classified in three classes 1, 2 and 3. class 1 with a range of $Af \geq 65$ or $Af \leq 35$ represents the high levels of basin tilt, or $57 \leq Af \leq 65$ represents the mean values of deviation and class 3 with a range of $43 \leq Af \leq 57$ represents the low values of basin tilt [10]. Consequently, the basin asymmetry map was prepared and produced by using Arc GIS 10.1 software (Fig. 6). The highest values of this indicator were measured in basins (3, 5, 6, 9, 10, 14, 15, 18, 19, 20, 22, 27, 28, 31, 34, 35, 37, 38 and 39).

3.3. Hyssometric and integral hypersonic curve (Hi)

Hypometric integral shows the distribution of altitude levels in a region and basin [30]. The Hi index describes the area of the lower surface of the hypersonic curve, thus indicating the capacity of an eroding basin. One of the simple methods for describing the shape of the hypsometric curve of a basin is to calculate its hypersometric integral.Hyssometric integral of the basin is obtained by using the area of the lower surface of the hypersometric curve. The equation used to calculate the hypersonic integral is as follows [8], [20]and [21]:

Hi = (Average elevation – min elevation / max elevation – min elevation).

In this index, the minimum, maximum and mean height were calculated from a digital elevation model (DEM) with accuracy of 30 m using Arc GIS version 10.1. After calculating the Hi index for all drainage basins, this index is classified in three classes [11]. Class 1 contains convex curves or kluge with an integral hypsometry greater than 0.5 (Hi≥0.5). This category of hypsometric curves with high values indicates the topography of the basin above its mean value. Class 2 contains convex-concave curves (0.4≤Hi0.5). This is the intermediate between class 1 and class 2. And Class 3 includes concave curves with hypsometric integral values less than (Hi0.4) 0.4, This category represents the cut off the net at levels with a mild topography than the first one. To form the hypsometric curve of a drainage basin, we plot the total height of the area in relation to the total area of the basin. Due to the fact that in the hypersonic curve, the area and height of the basin are divided into the total area and height of the basin, the numbers are dimensionless, Therefore, the hypsometric curves are independent of area and height. Therefore, these types of curves can be compared in each other in terms of size, height, and area. Hence, due to this feature of hypsometric curves, topographic maps can be used in different scales. The relationship between the hypersonic integral and the cutoff value of drainage networks is used as an indicator for determining the erosion cycle of landscapes in the region. This cycle occurs during several stages, which are: youth stage, puberty and aging.

The young stage in this cycle is characterized by deep cuts and uneven prominences. In the stage of puberty, we see a balance in geomorphologic processes. An aging stage is described with close-to-surface scenarios and very closely related prominences. Therefore, hypsometric curves, which are very important in posterior and vertical evaluation, are particular importance as an efficient method for identifying active and passive tectonic areas.

Hypersometry integrals have been measured in 40 studied areas. The minimum value of the measured hypsometric integral belongs to basin number 23 with the value (0.11), the shape of the curve for which it is concave, and the maximum value of this integral is obtained in domain number 7 with the value (0.55) and the convex curve. In Figure 7 according to the Hi level, the sub-basins are divided into three categories 1, 2, and 3, which respectively represent the high, middle and bottom tectonic activity.

As is clear from this form, the basins with activities 1 and 2 are located within the fault zones of Aladagh Leo, Kashk E Nosrat, Hasan Abad, Khasrud, Hajj Arabi, Korcheshmeh, Sari Dareh-Hajj Arabs. In general, a large part of the area shows a low activity category, indicating that the area studied has a low sensitivity to the hypsometric index. In other words, there is no significant difference in height between sub-basins.

3.4. Drainage Basin Form (Bs)

During the tectonic processes, the shape of the basin may change. The basin shape indicator, the difference between significant stretches of basins, and basin shapes that are close to the circle. The horizontal image of a basin can be described by the shape of the basin or the stretch ratio [25]. In regions that are active from the spectacle, the basins are taller and with high levels of this index and in areas with lower tectonic activity, the stretching of the basins decreases and their shape becomes closer to the circle and the value of Bs decreases [8].The drainage basin shape index (Bsc) is determined by using the following equation [25]and [9]:

Bs= Bl/Bw

In the above relation, the length of a basin in the main drainage path that is calculated from the point of drainage from the basin to the highest point in the basin, Bw is also the width of the basin, which is measured at the widest part of the basin, that is parallel to the length of the basin (Bl).

The Bs index for all basins was measured and the results were ranked in three classes, These 3 categories are: Category 1 tectonic activity (Bs≥4), Category 2 tectonic activity (3≤Bis4) and Category 3 tectonic activity (Bs≤3) [11]. The amount of tectonic activity in the first category is the highest and in the third category is the lowest. The results of calculating the Fbs index in 40 domains have been studied. The range of results for this indicator varies from 1.69 (range 19) to 11.35 (in domain 33). Approximately 60% of the studied basins are close to the circle and belong to class 3 tectonic activity. In the map derived from the measurement of the shape of the basin (Fig. 8), there are several focusing centers of the underlying basins.

Because the trapped sub-basins, which have the rank 1, represent tectonic activity in that basin, the focus of these sub-bases around a fault can be attributed to its quaternary activity of that fault. The highest concentration is under the drainage basins in the vicinity of Koshk E Nosrat, Hasrud, Hasanabad, Celery-Needles, Bidou, Korcheshmeh, Haj-Arab-Seminak, Moheb Ali, Eshtehard and Gheshlag Aladaghlu. In general, and according to the results of measurements of the drainage index of the basin, the activity of Kushn-E-Sassar and Hassan Abad faults has been much higher in the production of highly active and drained basins and indicates the greater activity of these faults than other faults in the studied area.

3.5. Width of Valley Valley to Valley Height (Vf)

This index is one of the morphometric indices that affects tectonic uplift and is sensitive to this factor. This indicator is defined as the ratio of the bottom of the valley to the valley height as follows:

Vf = Vfw/ [(Ald-Asc) + (Ard-Asc) /2)]

In the above relation (Vf) the ratio of width to valley height, (Vfw) Valley Width, (Asc), (Ald), (Ard) respectively, the height of the dividing line is in the right and left valleys and the bottom of the valley [8]. Normally, high values of the Ivf index are consistent with tectonic uplift rates [20]. After calculating the Vf index in the range of studies, this index is graded in three classes, the three classes are: class 1 (Vf≤0.5), this category of the Vf index represents V-shaped valleys, class 2 (0.5≤Vf1.0), this category of Vf represents an intermediate state of the valley between classes 1 and 3, and finally, class 3 (Vf≥1) represents U-shaped valleys [11]. The Vf index range in this study is varies from 2.65 (in basin 36) to 15.27 (in basin 16).

The results of measuring this index indicate that most of the valleys measured in the study area are U shaped. Figure 9: is mapping of sub-basins that is based on the Vf index in the study. As shown, according to the classification of this index, the area has U-shaped valleys.

3.6. The twist of Border between the Mountains and the Plains(Smf)

This index describes the equilibrium between river erosion processes that tend to cut into the border between the mountains and the plains and describes active tectonic forces that tend to produce a direct border between the mountains and the plains with fault [7]and [18]. This index is calculated by using the following equation [8]:

(J) (Smf) = Lj/Ls

In the above relation, Smf is the index of border between the mountains and the plains sinusitis, Lj is the length of the border between the mountains and the plains along the mountains, Ls is the length of the straight line of the border between the mountains and the plains.

This index is usually less than 3 and close to 1, with a steep sloping mountain suddenly rising along the border between the mountains and the plains [8]. High border between the mountains and the plains are directly and smoothly tectonic, and their value is low., but if the height of the border between the mountains and the plains elevation decreases or the upsurge is stopped, the border between the mountains and the plains is affected by erosion processes, its become sinusoidal shape and its screw rises, so, the value of the index J will also increase. Calculation of this index can be done by topographic maps or satellite imagery, Large-scale maps and high-resolution satellite-based satellite imagery can be used to accurately measure this indicator. This index has been surveyed for 31 border between the mountains and the plains and after calculating this index, it is classified in three tentative categories. In this categorization, category 1 J <1.10, category 2 1.50> J ≥ 1.10 and category 3 J ≥ 1.50 represents the tectonic activity of the region [11]. The lowest value of the index of the border between the mountains and the plains in this study is about 1 that is related to basins (0, 8, 15, 16, 18, 21, 24, 25, 26, 28, 30, 36) (Fig. 10).

3.7 Activated Particulate Land (IAT)

In most tectonic studies, the Activated Particulate Land index is evaluated by the two main indicators and studies often focus on the border between the mountains and the plains or river basins [7] and [5], [22] , [27]. In this study, a number of geomorphic indicators have been analyzed throughout the region to estimate tectonic activity, such as: Longitudinal gradient of the river, asymmetry of drainage basin, hypsometric integral, drainage basin shape ratio, the width of the valley to the height of the valley and the twist of border between the mountains and the plains indicator.

The relative active generation land (S / n) is obtained by using the mean values of each category of morphotectonic indices in all basins. To characterize the intensity and degree of tectonic activity, this index is distributed in 4 tectonic categories: category 1 Relative activated production (1.0≤Iat□1.5), this category represents a very high tectonic activity. Category 2 this index with an interval (1.5≤Iat□2.0), represents a relatively high tectonic activity. Category 3 activated particulate land index with values (2.0≤Iat□2.5), the average tectonic activity is shown and category 4 with a value of (2.5≤Iat) shows a relatively low tectonic activity.

Finally, after classifying the relative active tectonic values, the distribution map of the tectonic activity of the area was arranged in Arc GIS 10.1 software environment and the area of study was divided into four sections: very active, active, moderate activity and low activity area (Fig. 11). Analyzing the results of the classification of the relative active geochemical index that 30% of this study are very high and high tectonic activity in the region and located in the class 1 and 2 of the Iat index, and about 65% is in category 3, indicating moderate tectonic activity in the region. About 5% of the area study is in the category of 4 Iat indicators, which indicates low levels of tectonic activity in the studied area (Table1).

4. Discussion And Conclusion

- Based on Indes SL measurements, number basins (0, 5, 6, 8, 10, 12, 14, 15, 18, 19, 20, 21, 22, 23, 29, 33 and 35) have activity level 1 and show the highest SL rate. These basins are located on the faults of Aipak, Hasan Abad, Kooshk E Nosrat and Soltanieh. Activity level is 2 and have lower SL rate.
- The highest SL values were measured in basins (0, 6, 12, 22, and 29), which are influenced by the effects of Kooshk E Nosrat, Hassanabad, Aipak and Soltanieh faults. Because the rivers of the area are completely in line

with the fault zones, and on the other hand, in areas where we have no major flaws, the river with high SL is not seen, the results can be more trusted.

- Based on the results obtained from Af measurement, activity 1 basins are expanding in most areas, whether plain or in highlands. The focus of most of the 1st and 2rd basins is with the highest tilt around the main faults, such as Kooshk E Nosrat, Hassan Abad, Avaj, Aipak, which itself represents recent quaternary activities.
- An examination of the hypsometric index in the region, shows that a large part of the region has a low activity category and this suggests that this study had a low sensitivity to the hypsometric index, in other words, there is no significant difference in height between basins.
- According to the results of measuring the basin elongation index (Bs), the activity of Noshahr and Hasan Abad Cooke faults has been much more extensive in creating highly active and dragged basins, and the greater activity of these faults than other faults is studing.
- The results of calculating the Bs index in this study, show that approximately 60% of the studied basins are close to the circle and belong to class 3 tectonic activity.
- The classification of sub-basins based on the Vf index in this studied, shows that the area has U-shaped valleys.
- Examining the border between the mountains and the plains by Hill's picture and its elevation meters, show that the sub-basins that are adjacent to or along the main faults have the highest rate of J activity, also, the main focus of the active sub-basins is in terms of sinusoidal the border between the mountains and the plains along Kooshk E Nosrat, Hassan Abad, Avaj, Haj Arab Saminek, Soltanieh and Zanjan faults.
- Analyzing the results of the classification of the activated particulate land index shows that 30% of the study are very high tectonic activity in the region, located in class 1 and 2 of the Iat index, and about 65% is in category 3, indicating moderate tectonic activity in the region. About 5% of the study is also ranked in the fourth IAT mark, which indicates low levels of tectonic activity in the range.
- According to the study of the activated particulate land index in the studied area, Aladagh Lo faults, Eshtehard, Kooshk E Nosrat, Khoshkrud, Hassanabad, Aipak, Haj Arab Seminak, Moheb Ali, Bidou, Zardrang, Ahmad Abad Caravanserai, Karafs-Sozan, has very relative activity and Soltanieh faults-Darjezin, Zanjan, Abdareh, Avaj, Baqerabad have moderate relative tectonic activity. In the meantime, a fault with a relatively small tectonic activity is not observed, and in general, the entire zone can be considered as active tectonically.
- Out of the Indes measured indicators for the studied range, the AF, SL, and J indexes had the highest activity rates, indicating the sensitivity of these indices to the type of dominant movement in the zone. Nearly all of the zone faults are dominated by drift thrust, like the Kooshk E Nosrat's fault, the drift dominates with the slip component.
- Major and larg faults include Kooshk E Nosrat, Hassan Abad, Aipak, Khoshrud, Haj Arab Sinimak, and the basins corresponding to these faults, which include a large number of basin zones, all have a tectonic level of high or very high relative activity which indicates the high tectonic activity of these faults in the Quaternary. Kooshk E Nosrat and Hassan Abad fault and Haj Arab are the most important and most severe faults in the region, because almost all of the basins have high Iat.
- In Basin 18, where the bending of the Kooshk E Nosrat fault is to the southeast, the highest quaternary activity rate has been shown in all measured metrics.

References

1. Alavi M (1991) Sedimentay and Structural characteristics of the Paleo-Tethys remnants in northeastern Iran. GeolSoc of Amer Bull 103:983

2. Alavi M(1994) Tectonics of the Zagros orogenic belt of Iran: new data and interpretations: Tectonophysics, vol. 229, pp.211–238
3. Alavi M (1996) Tectonostratigraphic synthesis and structural style of the Alborz mountain system in northern Iran. J Geodyn 21:1–33
4. Altin T, Altin BN (2011) Development and morphometry of drainage network in volcanic terrain, Central Anatolia. Turkey Geomorphology 125:485–503
5. Azor A, Keller EA, Yeats RS (2002) Geomorphic indicators of active fold growth:South Mountain–Oak Ridge Ventura basin, Southern California. Geological Society ofAmerica Bulletin 114:745–753
6. Babaahmadi A, Safaei H, Yassaghi A, Vafa H, Naeimi A, Madanipour S (2010) A study of Quaternary structures in the Qom region, west central Iran. J Geodyn 50(5):355–367
7. Bull WB, McFadden LD(1977) Tectonic geomorphology north and south of the Garlock fault, CalifoQrnia, In: Doehring, D.O. (Ed.), Geomorphology in Arid Regions,Proceedings of the Eighth Annual Geomorphology Symposium, State University of NewYork, Binghamton, pp. 115–138
8. Bull WB(2007) Tectonic geomorphology of mountains: a newapproach to paleoseismology,Blackwell, Malden
9. Cannon PJ (1976) Generation of explicit parameters for a quantitative geomorphic study of Mill Creek drainage basin. Oklahoma Geology Notes 36(1):3–16
10. Dehbozorgi M, Pourkermani M, Arian M, Matkan AA, Motamedi H, Hosseiniasl A (2010) Quantitative analysis of relative tectonic activity in the Sarvestan area, central Zagros. IranGeomorphology 121(3):329–341
11. El Hamdouni R, Irigaray C, Fernandez T, Chacón J, Keller EA (2007) Assessment of relative active tectonics, southwest border of Sierra Nevada (southern Spain). Geomorphology 96:150–173
12. Hack JT(1957) Studies of longitudinal stream-profiles in Virginia and Maryland: U.S.Geological Survey Professional Paper 294B, 45–97
13. Hack JT (1973) Stream-profiles analysis and stream-gradient index. Journal of Research of the US Geological Survey 1:421–429
14. Hack JT(1982) Physiographic division and differential uplift in the piedmont and Blue Ridge. U.S. Geological Survey Professional Paper 1265, 1–49
15. Hack JT (1973) Stream-profiles analysis and stream-gradient index. Journal of Research of the US Geological Survey 1:421–429
16. Hack JT(1982) Physiographic division and differential uplift in the piedmont and Blue Ridge. U.S. Geological Survey Professional Paper 1265, 1–49
17. Hare PW, Gardner TW(1985) Geomorphic indicators of vertical neotectonism along converging plate margins, Nicoya Peninsula, Costa Rica. In: Morisawa, M., Hack, J.T
18. Keller EA (1986) Investigation of active tectonics: use of surficial Earth processes. In: Wallace RE (ed) Active tectonics Studies in Geophysics. National Academy Press, Washington DC, pp 136–147
19. Keller,E.and pinter,N.(1996)Active tectonics,Earth quakes,uplift and ,Earth sciencesseries,prentice-Hall,Newjersey
20. Keller EA, Pinter N (2002) Active Tectonics: Earthquakes, Uplift, and Landscape (2ndEd.) ". Prentice Hall, New Jersey
21. Mayer L (1990) Introduction to Quantitative Geomorphology. Prentice Hall, Englewood
22. Molin P, Pazzaglia FJ, Dramis F (2004) Geomorphic expression of active tectonics in a rapidly-deforming forearc, sila massif, Calabria, southern Italy. Am J Sci 304:559–589
23. Nabavi M H.(1355) A Preface to Iran's Geology, 109 p

24. Nowroozi AA, Mohajer-Ashjai A (1985) Fault movements and tectonics of Eastern Iran:boundaries of the Lut plate. GeophysJRastr Soc 83:215–237
25. Ramírez-Herrera MT (1998) Geomorphic assessment of active tectonics in the Acambay Graben, Mexican volcanic belt. Earth Surf Proc Land 23:317–332
26. Reddy GPO, Maji AK, Gajbhiye KS(2004) Drainage morphometry and its influence on landform characteristics in a basaltic terrain, Central India — a remote sensing and GIS approach, International Journal of Applied Earth Observation and Geo information 6, 1–16
27. Rockwell TK, Keller EA, Johnson DL(1985) Tectonic geomorphology of alluvial fans and mountain fronts near Ventura, California. In: Morisawa, M. (Ed.), Tectonic Geomorphology, Proceedings of the 15th Annual Geomorphology Symposium. Allen and Unwin Publishers, Boston, pp. 183–207
28. Silva PG, Goy JL, Zazo C, Bardajm T (2003) Fault generated mountain fronts in Southeast Spain: geomorphologic assessment of tectonic and earthquake activity. Geomorphology 250:203–226
29. Troiani F, Della Seta M (2008) The use of the stream length–gradient index in morphotectonic analysis of small catchments: a case study from Central Italy. Geomorphology 102:159–168
30. Strahler AN (1952) Hypsometric (area–altitude) analysis of erosional topography. Geol Soc Am Bull 63:1117–1142

Tables

Table 1: Tctonic activity value and category of morphotectonic indices in 40 drainage basins.

FID	Area	Af_Class	Bs_Class	Hi_Class	J_Class	SL_Class	Vf_Class	IAT	IAT_Class
0	1641/212524	2	3	3	1	2	-	2/2	3
1	545/702289	3	3	3	-	1	-	2/5	3
2	350/639366	3	3	3	-	1	-	2/5	3
3	317/617636	1	2	1	-	1	-	1/25	1
4	264/434992	2	3	2	-	1	-	2	3
5	358/599114	1	2	3	1	2	-	1/8	2
6	309/773686	1	3	3	-	2	-	2/25	3
7	241/304846	1	1	1	-	1	-	1	1
8	956/524916	3	1	3	1	2	-	2	3
9	944/198369	1	3	3	-	1	-	2	3
10	894/565547	1	3	3	-	2	-	2/25	3
11	343/786493	3	3	3	-	1	-	2/5	4
12	695/602212	2	3	3	1	2	3	2/33	3
13	364/197371	3	1	1	-	1	-	1/5	2
14	354/977416	2	1	3	-	1	-	1/75	2
15	654/506532	1	3	3	1	2	3	2/17	3
16	273/150224	2	3	3	1	1	3	2/17	3
17	366/708201	2	1	3	-	1	-	1/75	2
18	1008/171034	1	2	2	1	2	-	1/75	2
19	259/906074	1	3	3	2	2	3	2/33	3
20	474/495015	1	2	3	2	2	-	2	3
21	703/807133	2	3	3	1	2	-	2/2	3
22	625/493026	1	3	3	2	2	3	2/33	3
23	474/625188	3	2	3	-	2	3	2/17	3
24	382/191654	2	3	3	1	1	3	2/17	3
25	542/402432	2	3	3	1	1	3	2/17	3
26	566/700945	3	3	3	1	1	3	2/33	3
27	761/140952	1	1	3	2	1	-	1/6	2
28	516/578575	1	1	3	1	1	3	1/67	2
29	1058/94507	2	3	3	2	2	-	2/4	3

30	711/359588	3	2	3	1	1	3	2/17	3
31	372/03493	1	3	3	-	1	-	2	3
32	599/493474	3	3	3	-	1	-	2/5	4
33	289/064927	3	1	3	-	2	-	2/25	3
34	303/544527	1	3	2	-	1	-	1/75	2
35	458/759999	1	3	3	-	2	-	2/25	3
36	524/985544	3	3	3	1	1	3	2/33	3
37	287/044444	1	2	3	-	1	-	1/75	2
38	622/446328	1	3	3	-	1	-	2	3
39	324/15426	1	1	3	-	1	-	1/5	2

Figures

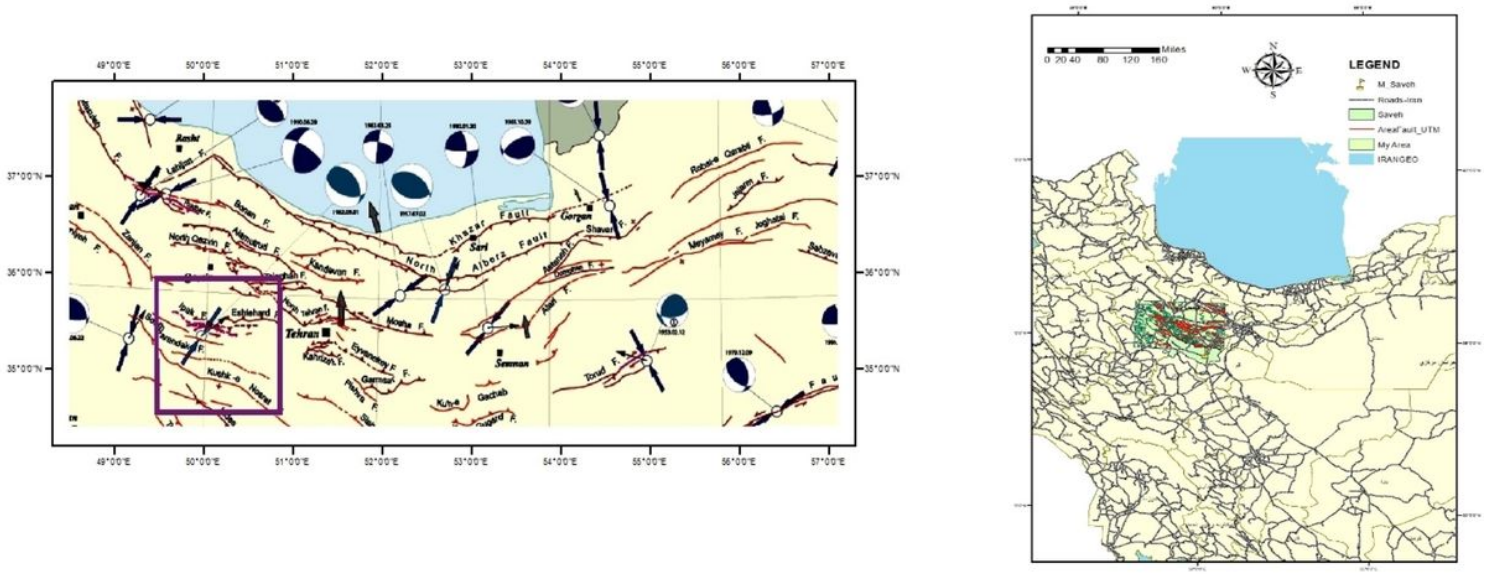

Figure 1

(1-1): Geolocation of the region (Hesami Azar et al.,2003). (1-2): Access roads to the region Note: The designations employed and the presentation of the material on this map do not imply the expression of any opinion whatsoever on the part of Research Square concerning the legal status of any country, territory, city or area or of its authorities, or concerning the delimitation of its frontiers or boundaries. This map has been provided by the authors.

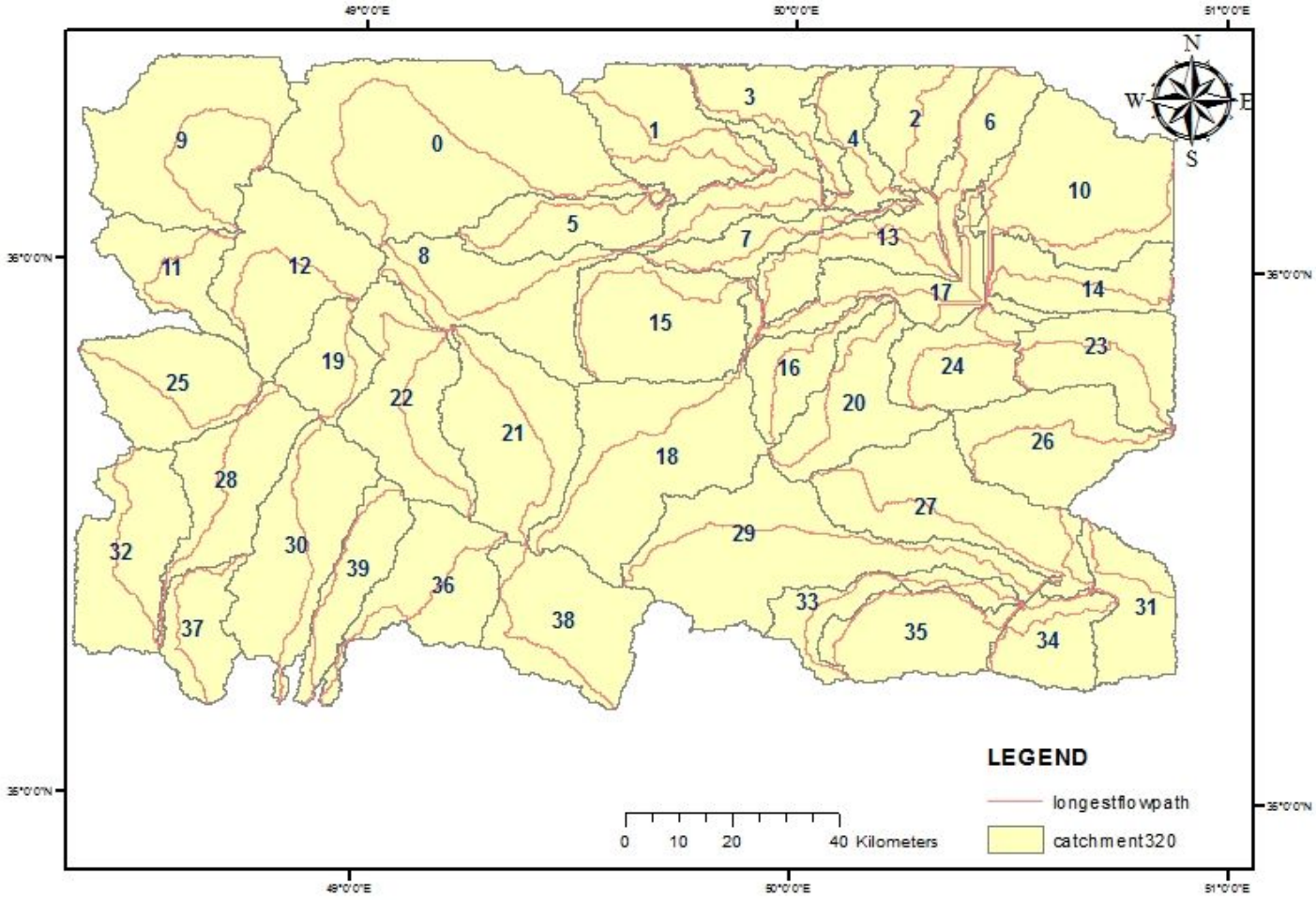

Figure 2

Drainage basins that created in this study area Note: The designations employed and the presentation of the material on this map do not imply the expression of any opinion whatsoever on the part of Research Square concerning the legal status of any country, territory, city or area or of its authorities, or concerning the delimitation of its frontiers or boundaries. This map has been provided by the authors.

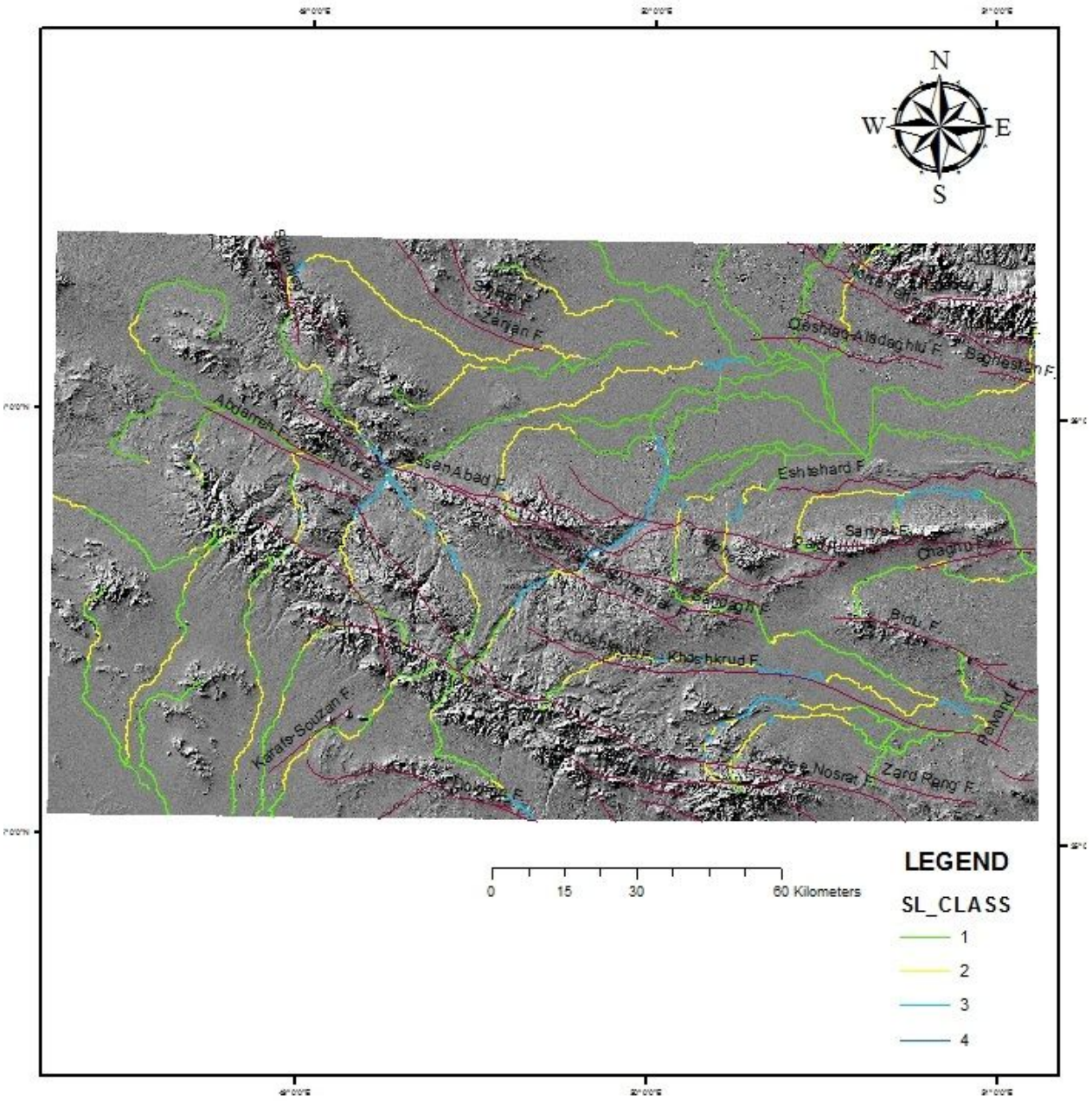

Figure 3

Classification of extracted waterways from the digital elevation model of the study area Note: The designations employed and the presentation of the material on this map do not imply the expression of any opinion whatsoever on the part of Research Square concerning the legal status of any country, territory, city or area or of its authorities, or concerning the delimitation of its frontiers or boundaries. This map has been provided by the authors.

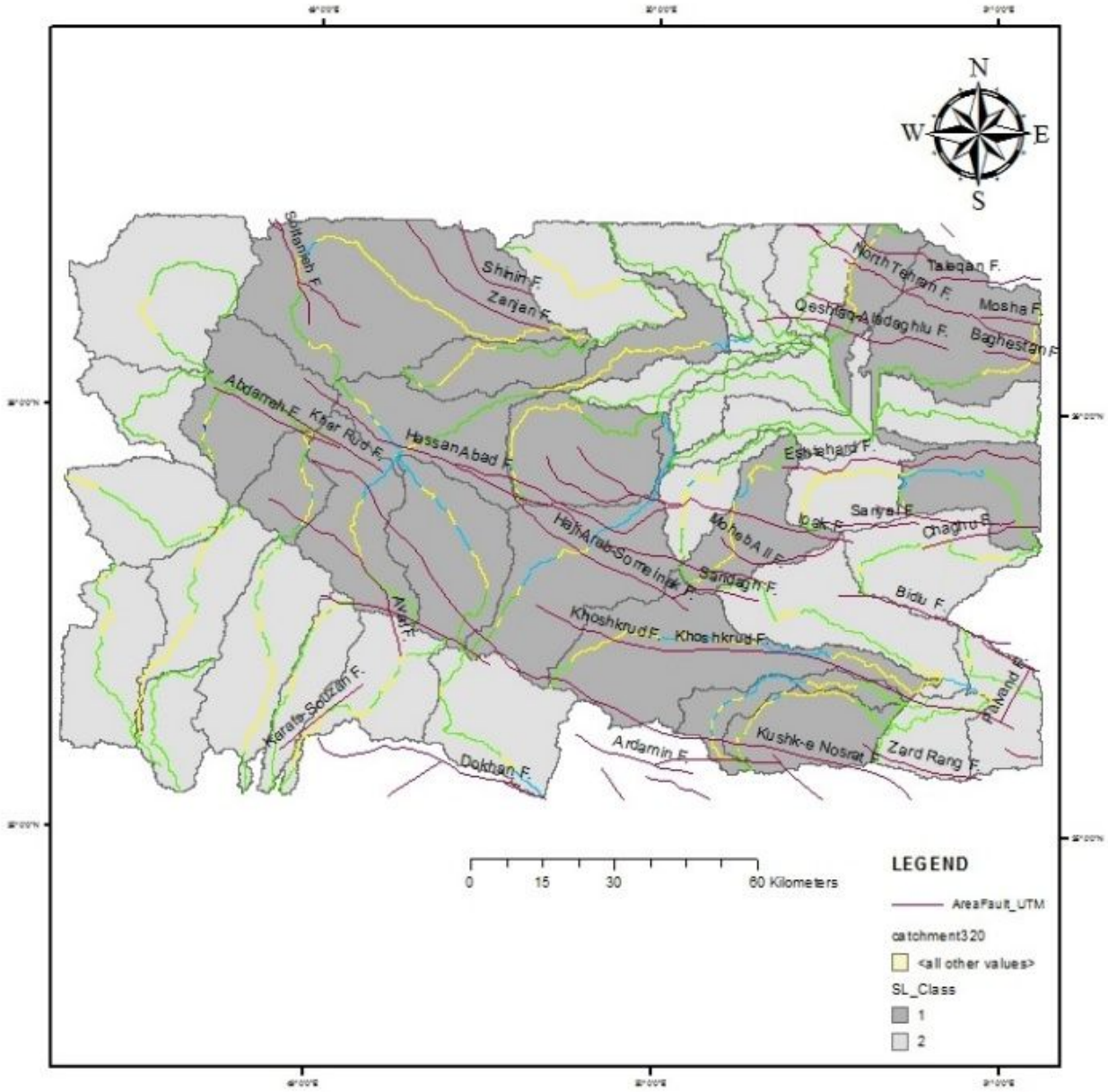

Figure 4

SL index map on a wide-ranging digital elevation model Note: The designations employed and the presentation of the material on this map do not imply the expression of any opinion whatsoever on the part of Research Square concerning the legal status of any country, territory, city or area or of its authorities, or concerning the delimitation of its frontiers or boundaries. This map has been provided by the authors.

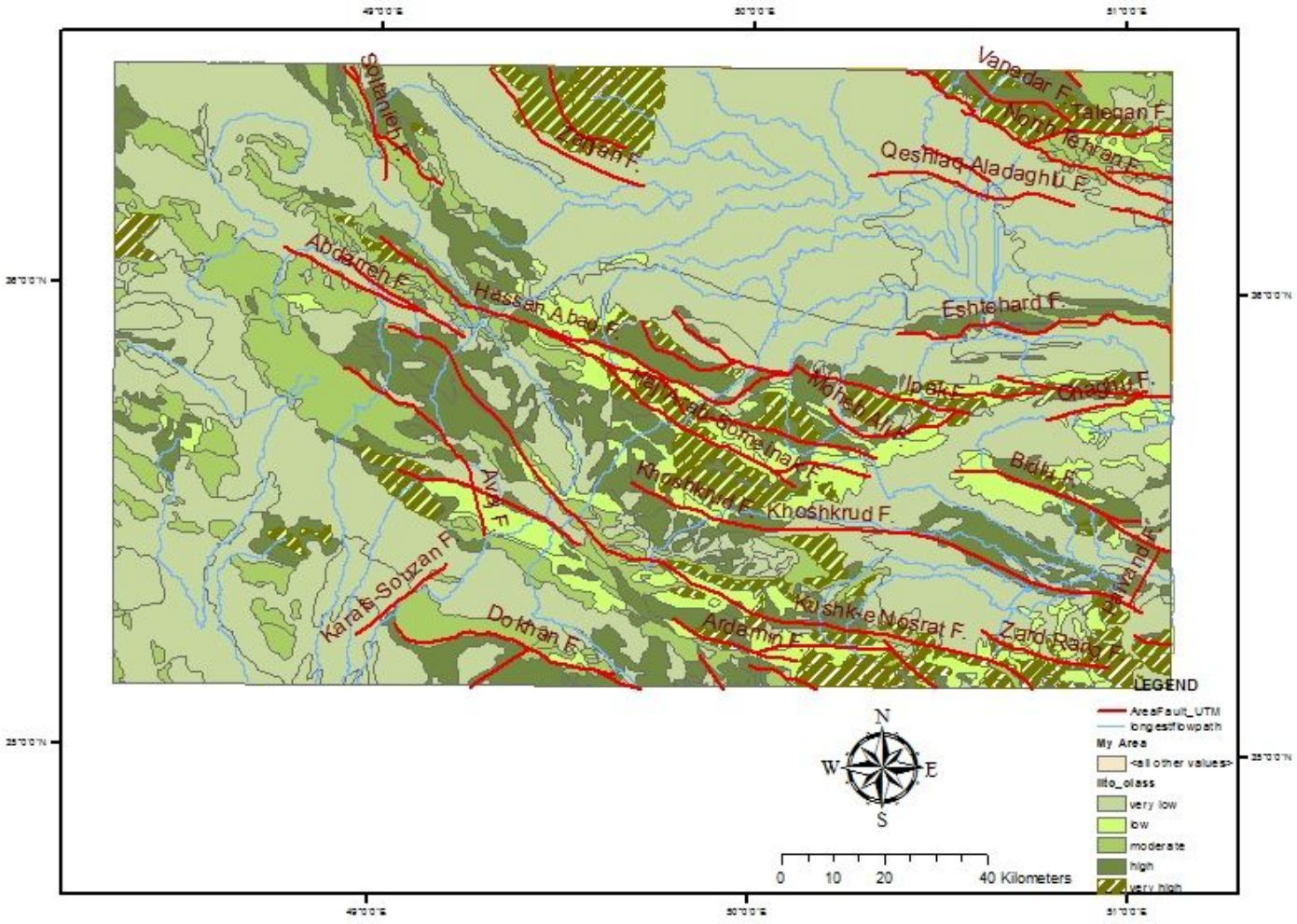

Figure 5

Distribution Map of SL Index Anomaly Values on Different Resistance Stones Note: The designations employed and the presentation of the material on this map do not imply the expression of any opinion whatsoever on the part of Research Square concerning the legal status of any country, territory, city or area or of its authorities, or concerning the delimitation of its frontiers or boundaries. This map has been provided by the authors.

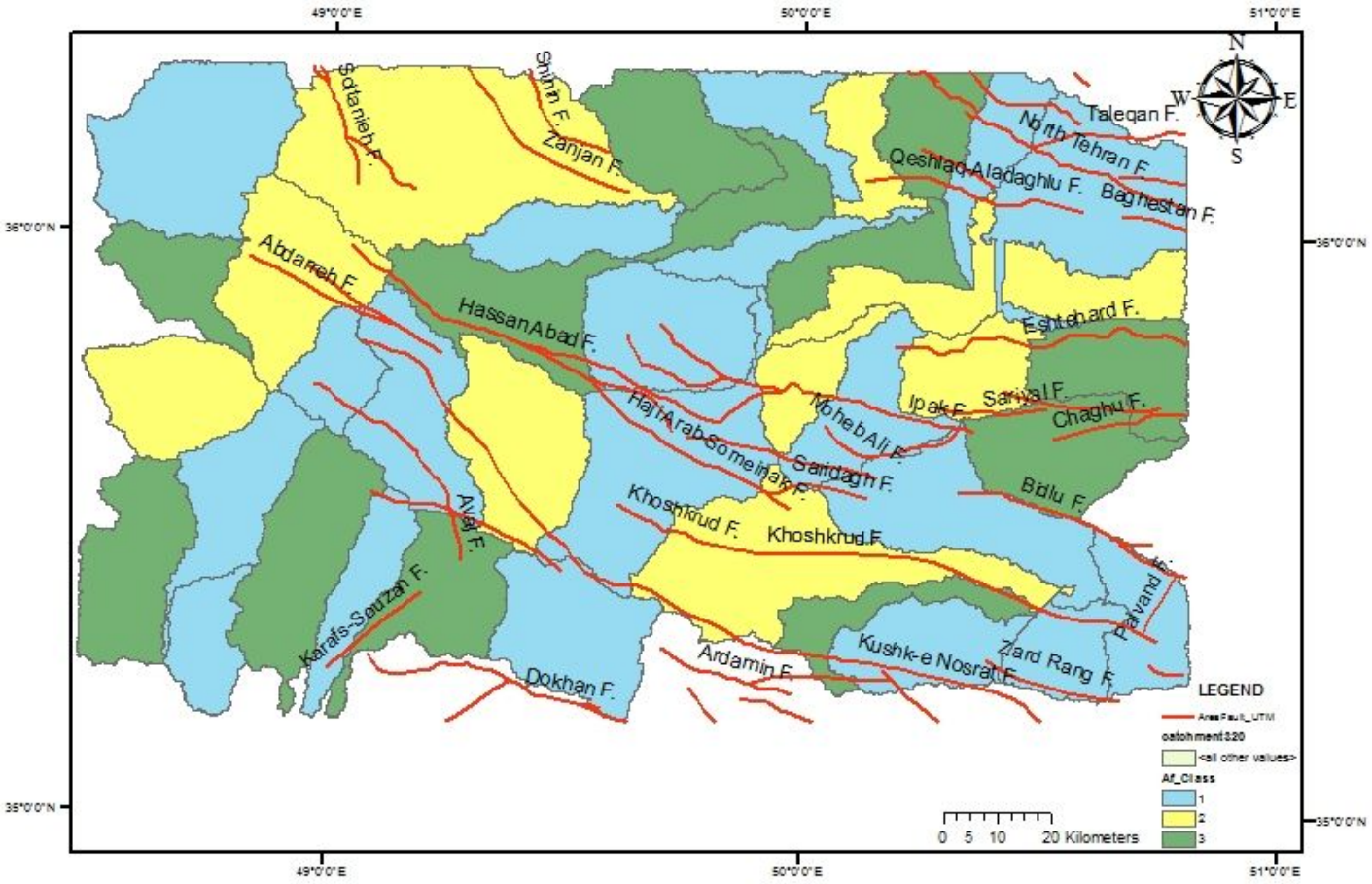

Figure 6

Drainage basin asymmetry map in the study area Note: The designations employed and the presentation of the material on this map do not imply the expression of any opinion whatsoever on the part of Research Square concerning the legal status of any country, territory, city or area or of its authorities, or concerning the delimitation of its frontiers or boundaries. This map has been provided by the authors.

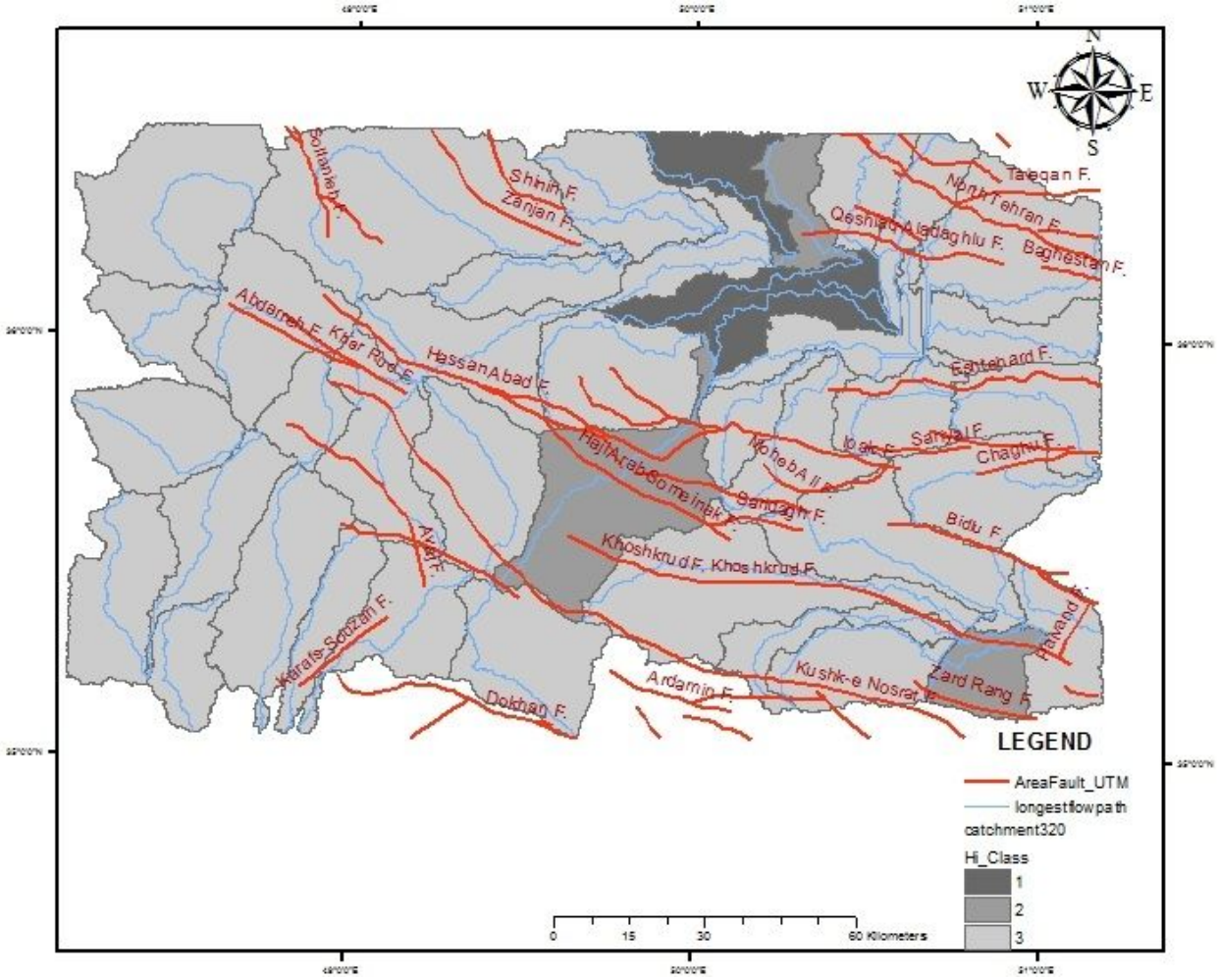

Figure 7

Sub-basin classification map based on the Hi index in the study area. Note: The designations employed and the presentation of the material on this map do not imply the expression of any opinion whatsoever on the part of Research Square concerning the legal status of any country, territory, city or area or of its authorities, or concerning the delimitation of its frontiers or boundaries. This map has been provided by the authors.

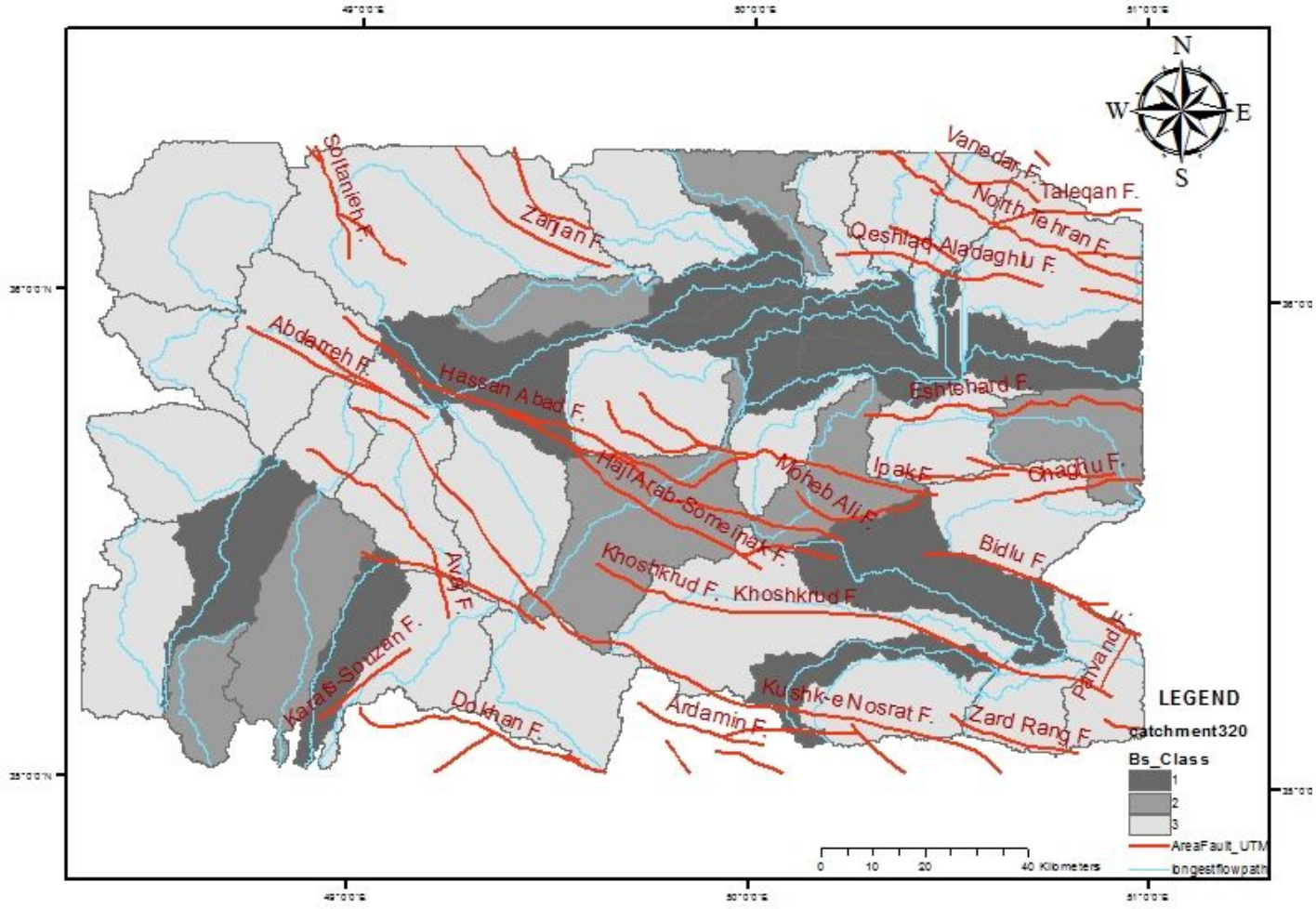

Figure 8

Sub-basin classification map based on the Bs index in the study area. Note: The designations employed and the presentation of the material on this map do not imply the expression of any opinion whatsoever on the part of Research Square concerning the legal status of any country, territory, city or area or of its authorities, or concerning the delimitation of its frontiers or boundaries. This map has been provided by the authors.

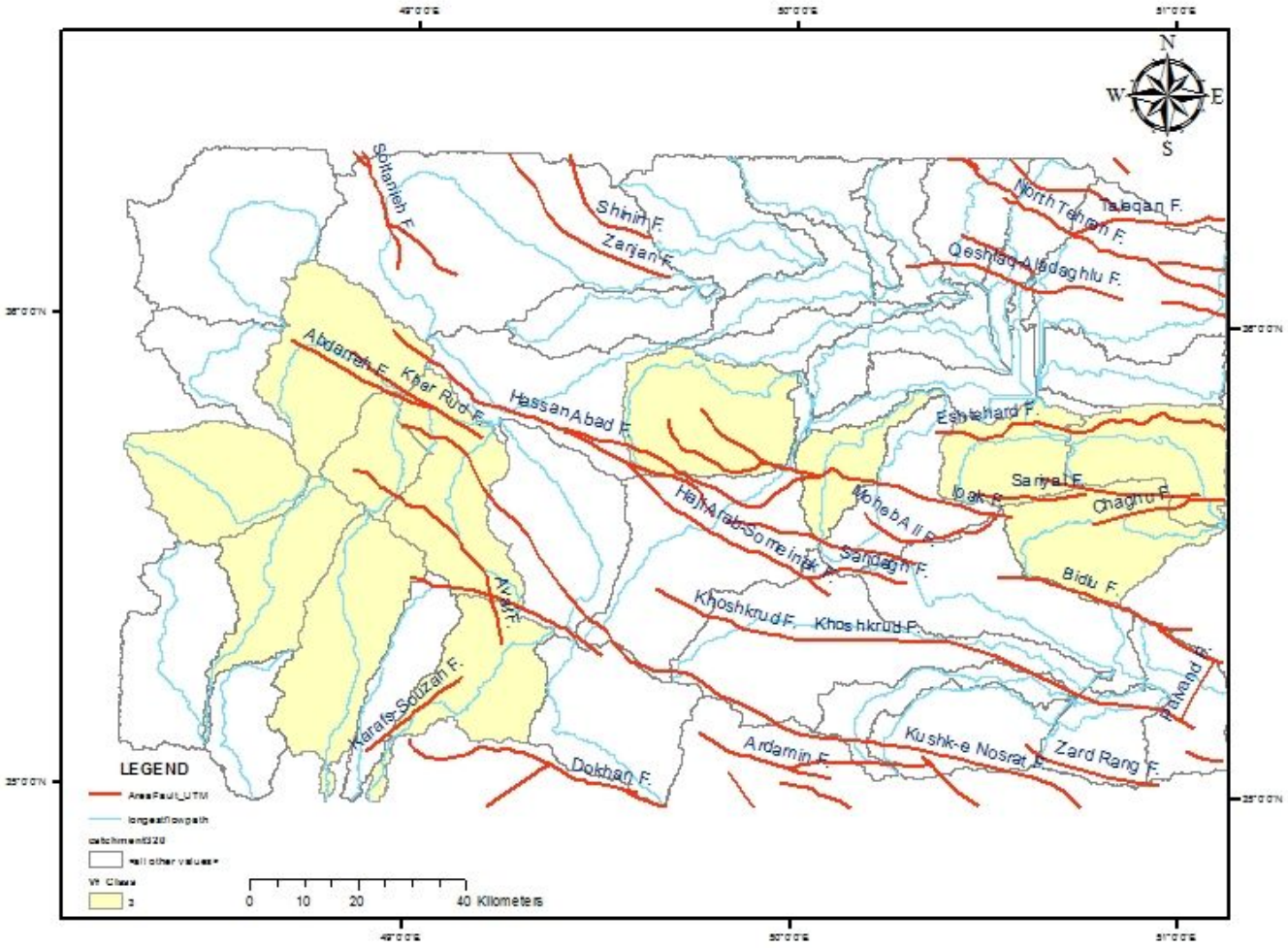

Figure 9

Sub-basin classification map based on the Vf index in the studied area. Note: The designations employed and the presentation of the material on this map do not imply the expression of any opinion whatsoever on the part of Research Square concerning the legal status of any country, territory, city or area or of its authorities, or concerning the delimitation of its frontiers or boundaries. This map has been provided by the authors.

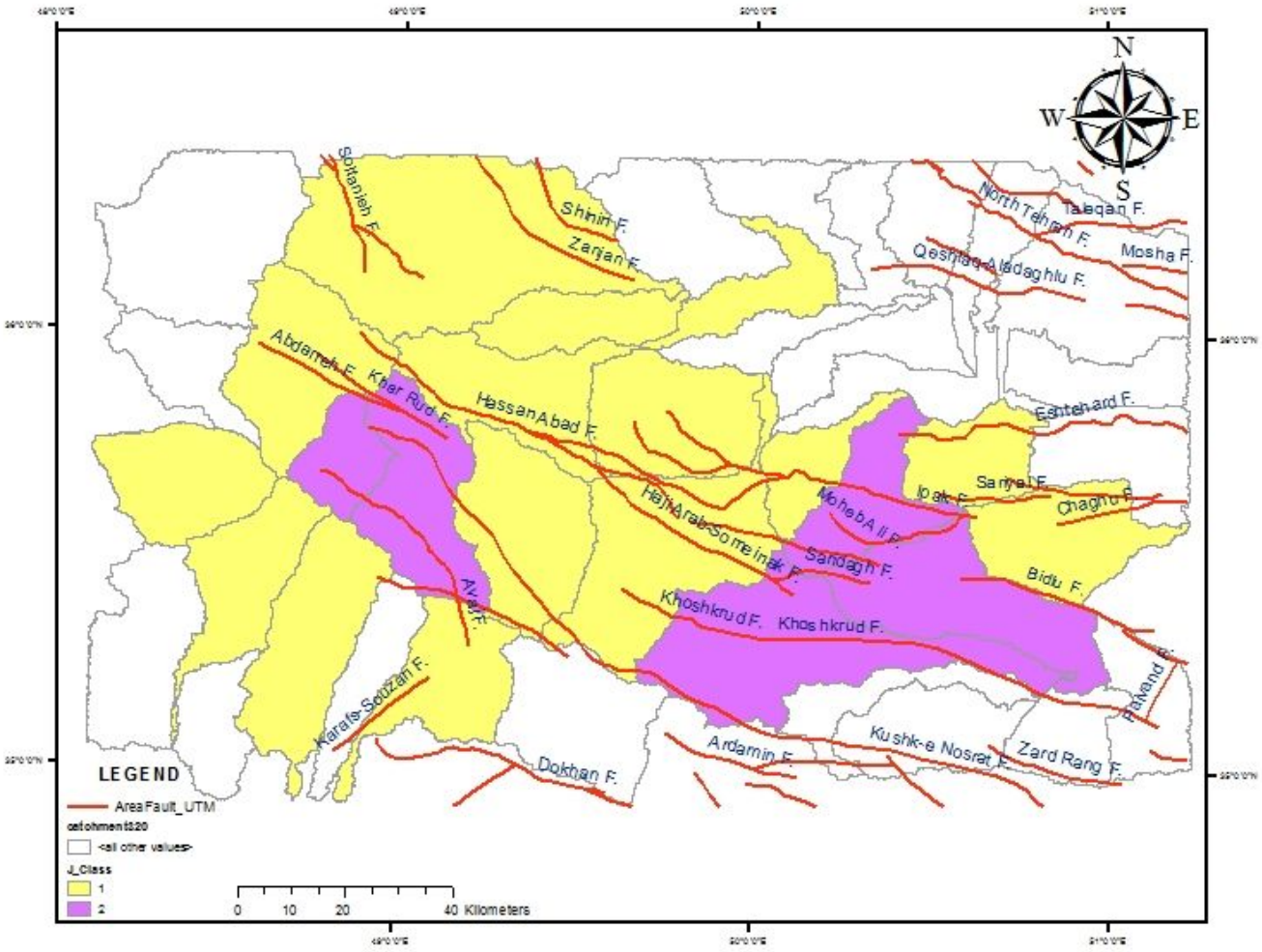

Figure 10

Sub-basin classification map based on the index of the J-mountain the border between the mountains and the plains index. Note: The designations employed and the presentation of the material on this map do not imply the expression of any opinion whatsoever on the part of Research Square concerning the legal status of any country, territory, city or area or of its authorities, or concerning the delimitation of its frontiers or boundaries. This map has been provided by the authors.

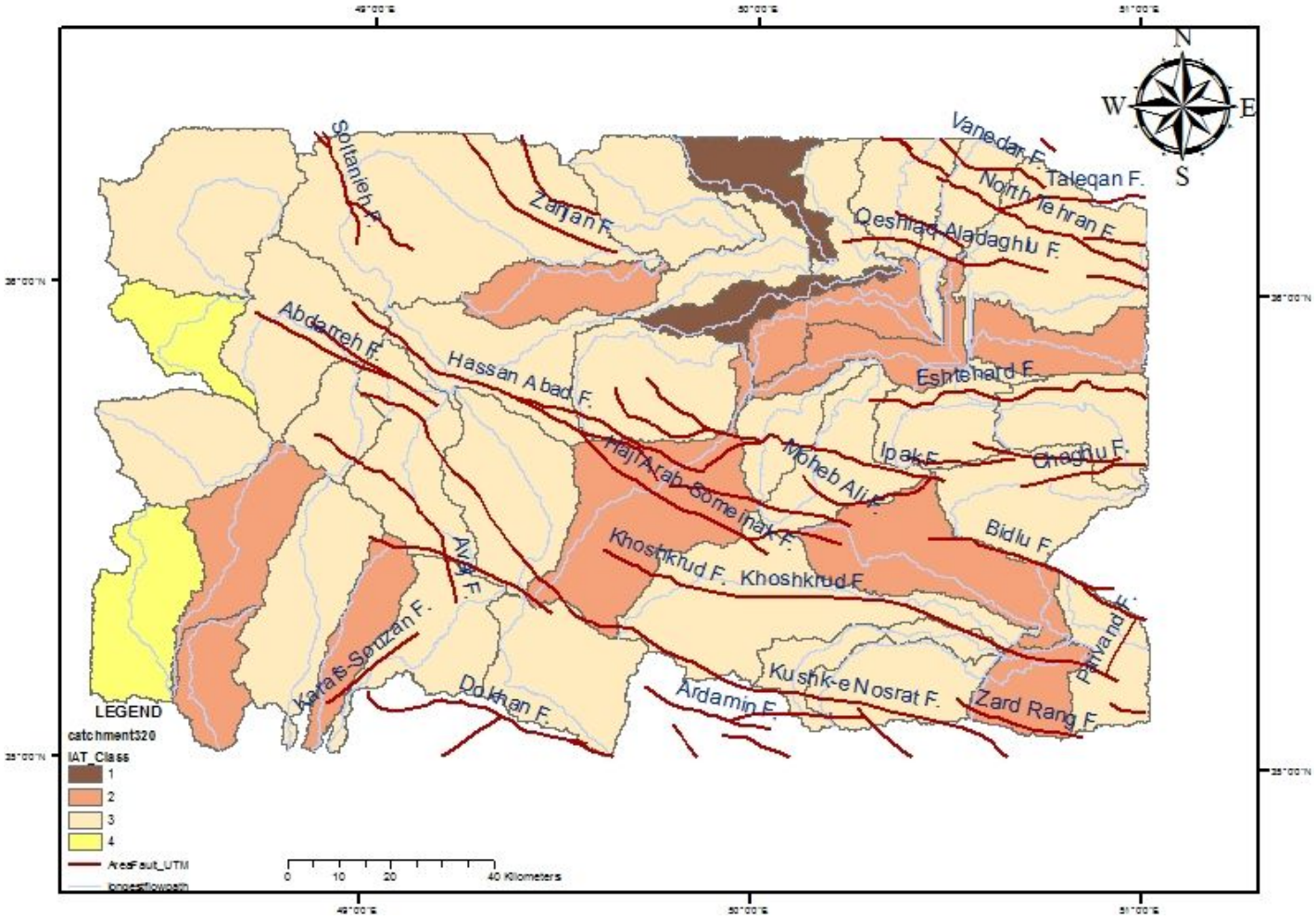

Figure 11

Relative tectonic activity level (Iat) distribution map in the study area. Note: The designations employed and the presentation of the material on this map do not imply the expression of any opinion whatsoever on the part of Research Square concerning the legal status of any country, territory, city or area or of its authorities, or concerning the delimitation of its frontiers or boundaries. This map has been provided by the authors.